JOURNAL OF BACTERIOLOGY, Aug. 1983, p. 565–577
0021-9193/83/080565-13$02.00/0

Vol. 155, No. 2

Genetics of Methyl-Accepting Chemotaxis Proteins in *Escherichia coli*: Organization of the *tar* Region

MARY K. SLOCUM AND JOHN S. PARKINSON*
Biology Department, University of Utah, Salt Lake City, Utah 84112

Received 1 March 1983/Accepted 9 May 1983

The *tar* locus of *Escherichia coli* specifies one of the major species of methyl-accepting proteins involved in the chemotactic behavior of this organism. The physical and genetic organization of the *tar* region was investigated with a series of specialized λ transducing phages and plasmid clones. The *tar* gene was mapped at the promoter-proximal end of an operon containing five other chemotaxis-related loci. Four of those genes (*cheR*, *cheB*, *cheY* and *cheZ*) are required for all chemotactic responses; consequently, polar mutations in the *tar* gene resulted in a generally nonchemotactic phenotype. The fifth gene, *tap*, was mapped between the *tar* and *cheR* loci and specified the production of a 65-kilodalton methyl-accepting protein. Unlike the *tar* locus, which is required for chemotaxis to aspartate and maltose, mutants lacking only the *tap* function had no obvious defects in chemotactic ability. Genetic and physical maps of the *tar-tap* region were constructed with Mu d1 (Ap^r *lac*) insertion mutations, whose polar properties conferred a phenotype suitable for deletion mapping studies. Restriction endonuclease analyses of phage and plasmid clones indicated that all of the genetic coding capacity in the *tar* region is now accounted for.

Chemotactic behavior in *Escherichia coli* represents a simple sensory transduction system that is readily amenable to genetic and biochemical analyses. In the absence of chemotactic stimuli, motile cells swim in random walk fashion by alternating episodes of clockwise and counterclockwise flagellar rotation (1, 30). Chemotactic movements are brought about by modulating the relative probabilities of clockwise and counterclockwise rotation in response to temporal changes in attractant or repellent concentration (18). These chemotactic responses exhibit two distinct phases: a rapid excitation event that initiates changes in flagellar rotation, and a subsequent adaptation process that produces a slow return to the prestimulus rotational pattern (2, 19, 28, 37).

Several transmembrane signaling proteins known as methyl-accepting chemotaxis proteins (MCPs) play key roles in both the excitation and adaptation phases of chemotactic responses (35). On the outer face of the membrane, the MCPs interact either with chemoeffector molecules directly (e.g., aspartate and serine) or with occupied chemoeffector binding proteins (e.g., maltose-, galactose-, and ribose-binding proteins), thereby generating signals that trigger changes in flagellar rotation (10, 14, 16, 41). After initiating a flagellar response, the MCPs undergo changes in methylation state that result in sensory adaptation (35). These methylation-demethylation reactions take place on the cytoplasmic side of the membrane and involve several glutamic acid residues in each MCP molecule (4, 6, 8, 9, 13, 40). The reactions are catalyzed by two MCP-specific enzymes, a methyltransferase specified by the *cheR* gene, and a methylesterase specified by the *cheB* gene (36, 38). Neither the nature of MCP signals nor the way in which methylation regulates those signals is yet understood in molecular terms.

The cell's major species of MCP, MCPI and MCPII, are products of the *tsr* and *tar* genes, respectively (31, 34). Genetic studies have shown that both of these components are responsible for processing a variety of sensory inputs: *tsr* mutants exhibit missing or defective responses to serine and related attractants (26), to indole, leucine, acetate, and other repellents (12, 39), and to temperature stimuli (20); *tar* mutants fail to respond to the attractants aspartate and maltose and to divalent cation repellents (26).

It should be possible to demonstrate the multifunctional nature of MCPs at the genetic level by obtaining MCP mutants specifically defective in stimulus detection, signaling, or methylation. Such mutants would also be extremely helpful in attempting to understand the biochemical properties of MCP molecules; however, only a few

MCP mutants have been described, and none has yet been subjected to detailed genetic analysis (10, 26).

This article is the first in a series of studies on the genetics of the major MCP loci in *E. coli*. In it we describe the genetic and physical organization of the *tar* region, including a fine-structure map of the *tar* gene, and demonstrate that *tar* is part of an operon containing other chemotaxis-related genes. We also present evidence for the existence of a "cryptic" MCP locus adjacent to *tar* and discuss some of its unusual properties. This new MCP locus has also been discovered independently by two other groups (3, 42), but opinions differ as to what functional role, if any, it plays in *E. coli*.

MATERIALS AND METHODS

Bacterial strains. The strains used in this work were derivatives of *E. coli* K-12; their properties are summarized in Table 1. The *tar* and *che* mutations listed in Table 1 were transferred from their original strains into RP437, RP4368, and various other genetic backgrounds by cotransduction with the *eda* locus, as previously described (22). The resulting recombinant strains are not listed in Table 1, but rather are discussed below. Other strains not listed in Table 1 included a large number of *che* mutants from our strain collection (22, 23) that were used in mapping tests to determine the genetic content of plasmids and specialized transducing phage.

Phage strains. Phage P1 *kc* was used for generalized transduction. Specialized transducing phage λfla52 (*tar*$^+$) and λfla52Δ1 (*tar*$^-$) were obtained from M. Silverman, University of California at San Diego (32). Derivatives of λfla52 carrying polar *tar* mutations (*che-235*, *che-252*) were constructed by first lysogenizing strains RP4338 (*che-235*) and RP4339 (*che-252*) with λfla52Δ1, which has no attachment site and must form lysogens by homologous recombination. The resulting lysogens were heat induced at 42°C to produce a lysate containing a mixture of λfla52Δ1 parental phage and recombinants carrying the polar *tar* alleles. Recombinant and parental phages were separated by equilibrium banding in CsCl density gradients, the denser phage, which had lost the *tar* deletion of λfla52Δ1, were checked for the polar *tar* point mutation by complementation and mapping tests with other *tar* point mutations. Deletion derivatives of λche22

TABLE 1. Bacterial strains[a]

Strain	Relevant markers[b]	Comments	Reference or source
RP437	*eda-50*	Standard background for introduction of *eda*-linked chemotaxis mutations	(25)
RP4368	*tsr-1 eda-50*	Construction of *tar tsr* doubles	(24)
RP3098	Δ(*flbB-flaH*)*4*	Host for growth of λ stocks	(33)
RP511	*rho-104 eda-50*	Recipient for polarity tests	This work
RP3030	*uvrA* (λ *ind*$^-$)	UV programming host	(33)
5K	*hspR*	Recipient in plasmid constructions	N. Murray
RP3808	Δ(*cheA-cheZ*)*2209 tsr-1*	Host for phage mapping crosses	This work
YK410	Δ*lacU169*	Parent of *mud* mutants m1 through m299	(15), Y. Komeda
RP506	Δ*lacU169 eda-50*	Parent of *mud* mutants m300 through m399	This work
MAL103	Mu, Mu *d*1 (Ap^r, *lac*) lysogen	Preparation of *mud* donor lysates	(5) Y. Komeda
RP4362	*che-226 eda*$^+$	Polar *tar* allele	(23)
RP4308	*che-229 eda*$^+$	Polar *tar* allele	(23)
RP4338	*che-235 eda*$^+$	Polar *tar* allele	(23)
RP4339	*che-252 eda*$^+$	Polar *tar* allele	(23)
RP4340	*che-256 eda*$^+$	Polar *tar* allele	(23)
RP4446	*tar-1 eda*$^+$	Original *tar* mutant background	(26) J. Adler
RP4447	*tar-2 eda*$^+$	Original *tar* mutant background	(26) J. Adler
RP4448	*tar-3 eda*$^+$	Original *tar* mutant background	(26) J. Adler
RP4449	*tar-4 eda*$^+$	Original *tar* mutant background	(26) J. Adler
RP4450	*tar-5 eda*$^+$	Original *tar* mutant background	(26) J. Adler
RP4451	*tar-6 eda*$^+$	Original *tar* mutant background	(26) J. Adler
RP4445	*tar-8 eda*$^+$	Original *tar* mutant background	(26) J. Adler
RP4606	*cheW113*	Recipient for Δ*tar-5201* transfer	(23)

[a] Other strains used in this work were derived from these by P1 transductions or Mu *d*1 mutagenesis, as described in the text.

[b] All of these strains carry additional mutations, particularly auxotrophic markers, that are not relevant to the work described here.

(25) were used for fine structure mapping of *tar* mutations and for gene product identification. Their genetic content is shown in Fig. 4. Recombinant λche22 strains with two deletions were constructed by phage crosses in strain RP3098 and are listed in Table 3.

Media. Unless otherwise noted, all experiments were carried out in tryptone broth, tryptone agar, or tryptone semisolid (swarm) agar (22) at 35°C or, in the case of Mu *d*1(Ap^r, *lac*) (herein described as Mu *d*1) experiments, at 30°C. Nutritional selections were done on H1 minimal medium as described previously (22). Phage stocks were prepared in liquid NZ-amine medium as described by Parkinson and Houts (25).

Transfer of Δ *tar-5201* to the *E. coli* chromosome. λfla52Δ1 was irradiated with UV light from a 15-W germicidal lamp (approximately 1,200 ergs per mm^2) and used to infect strain RP4606 at a multiplicity of 0.1. The infected cells were streaked across the surface of a tryptone swarm plate and incubated overnight at 30°C. Recombinant swarms that had rescued the *cheW*$^+$ allele from λfla52Δ1 were picked, cloned at 42°C to eliminate lysogens, and tested for aspartate taxis on tryptone swarm agar. Approximately three-fourths of the tested swarms appeared to have inherited the *tar* defect from λfla52Δ1. One such strain was chosen for use as a transductional donor to introduce the *tar* mutation (designated Δ*tar-5201*) into strain RP437.

Isolation of insertion mutations. Mu *d*1 lysates were prepared from strain MAL103 as described by Casadaban and Cohen (5). Mu *d*1 transductants of strains RP501 and RP506 were selected on ampicillin medium, and pools containing approximately 1,000 transductant colonies were screened for chemotaxis mutants by the "miniswarm" method (22). Each independent chemotaxis mutant obtained from the miniswarm screen was then subjected to P1 transductional crosses to verify that they contained only a single Mu *d*1 prophage that was 100% linked to the chemotaxis defect.

Mapping methods. Complementation and recombination tests with specialized transducing phages were done by the low-resolution and high-resolution methods described previously (25, 33). Both methods utilize tryptone swarm agar to recognize rare chemotactic recombinants among a large number of infected Che$^-$ cells. In some cases deletion endpoints in the transducing phages were mapped relative to one another by phage crosses in strain RP3808, which carries a large deletion across the *tar* operon. Although this host strain could not recombine with either phage parent, its chemotaxis defect could be corrected through the formation of an appropriate recombinant phage. Crosses were performed at a multiplicity of 5 for each parental phage. After a 20-min adsorption period, approximately 10^8 infected cells were streaked across the surface of a tryptone swarm plate to score for the production of Che$^+$ recombinants.

Construction and mapping of plasmids. Approximately 100 μg of pBR322 DNA was digested to completion with restriction endonuclease *Sal*I, which cuts the circular plasmid at one site. The linearized DNA was divided into two samples; one was treated with *Eco*RI, and the other was treated with *Bam*HI. The larger fragment from each reaction was purified by sucrose gradient centrifugation, yielding two types of vector DNAs with heterologous ends. Donor DNA fragments were generated by digesting 10 μg of λche22 DNA with a combination of either *Eco*RI-*Sal*I or *Bgl*II-*Sal*I and then ligated to the appropriate vector fragment (*Bam*HI and *Bgl*II produce homologous single-stranded ends). Strain 5K was transformed with the ligation mixtures by the $CaCl_2$ procedure, selecting for ampicillin-resistant colonies and then screening for tetracycline sensitivity. Plasmid DNA was prepared from each of 24 transformant colonies from each ligation reaction and analyzed by restriction mapping to identify the insert in each.

The genetic content of each recombinant plasmid was determined by recombination tests with a series of *mot* and *che* host strains. Plasmid DNA was transferred into the tester strains either by transformation or by P1 transduction with identical results. The ampicillin-resistant recombinants were transferred to tryptone swarm plates to detect formation of Che$^+$ or Mot$^+$ recombinants.

Restriction mapping of phage and plasmid DNA. DNA was isolated from CsCl-banded λ particles by the formamide method (7). Plasmid DNA was extracted by the method of Ish-Horowicz and Burke (11). DNA was digested with enzymes obtained from either New England Biolabs or Bethesda Research Laboratories, under the conditions recommended by the enzyme supplier. Digested samples were run on 1% agarose gels and analyzed by methods previously described (7).

Analysis of chemotaxis-related gene products. λche22 transducing phages were used to label specifically chemotaxis gene products by UV programming as described previously (33). Samples were analyzed in sodium dodecyl sulfate-containing polyacrylamide gels by the Laemmli method (17).

RESULTS

Cotranscription of *tar* and *che* genes. The *tar* locus lies near a cluster of four *che* genes in the order: *tar cheR cheB cheY cheZ*. Boyd et al. (3) recently reported that insertions of transposon Tn*5* at the *tar* locus blocked expression of the *cheRBYZ* functions. Previous work had shown that these four *che* loci were cotranscribed in the *cheR-cheZ* direction, so the Tn*5* observations could be explained as a polar effect, if the *tar* gene were part of the *cheRBYZ* transcriptional unit (23). Alternatively, the *tar* function itself might be required for *cheRBYZ* expression. To distinguish these two possibilities, we examined the chemotaxis and complementation properties of two groups of mutants. The first group carried polar (Che$^-$) mutations that had been previously mapped to the *tar-cheR* region. Complementation analysis and fine structure mapping of these mutations showed that they were located in the *tar* gene. The second set of mutant strains carried the *tar* alleles described by Reader et al. (26). We found that some of these *tar* mutations had polar properties. These findings indicate that the *tar* gene is cotranscribed with the *cheRBYZ* genes, with the promoter for this operon located next to the *tar* locus. Below we

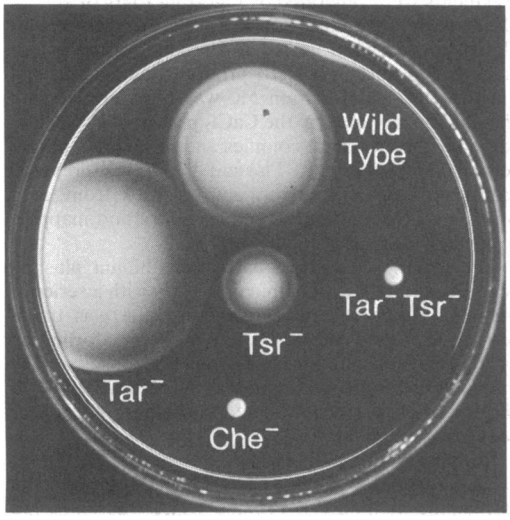

FIG. 1. Swarm phenotypes of chemotaxis mutants. A tryptone swarm plate was inoculated with individual colonies of RP437 (Che$^+$, wild type) and RP437 derivatives carrying the mutant alleles Δ*tar-5201* (Tar$^-$), *tsr-1* (Tsr$^-$), Δ*tar-5201 tsr-1* (Tar$^-$ Tsr$^-$), and *cheY223* (Che$^-$). The plate was incubated at 35°C for 10 h.

present the evidence in support of this conclusion.

On semisolid tryptone agar swarm plates, chemotactically wild-type strains such as RP437 form large colonies with several discrete rings that represent bands of migrating cells (Fig. 1). The outermost ring is due to chemotaxis toward serine, whereas the complex inner ring is produced by a combination of aspartate taxis and oxygen taxis. The canonical Tar swarm phenotype is best illustrated by RP4324, which carries the Δ *tar-5201* deletion mutation. This strain forms large swarms that lack the inner ring (Fig. 1). By contrast, strains defective in any of the *che* functions form very small colonies with no evidence of chemotactic rings (Fig. 1). These observations tend to rule out the possibility that *tar* function is directly required for *che* gene expression, because the *tar* null mutation Δ*tar-5201* does not exhibit a Che$^-$ phenotype. However, if the *tar* and *che* loci were cotranscribed, polar mutations in *tar* would produce a Che$^-$ phenotype.

We examined five ethyl methane sulfonate-induced *che* mutations (allele numbers *226, 229, 235, 252* and *256*) that were mapped in the *tar-cheR* region and had polar effects on *cheRBYZ* expression. The nature of the polar lesions is not known, although none of these mutations responded to amber suppressors. Nevertheless, it seemed likely that their polar effects would be dependent on Rho factor, which is required for most types of transcription termination. We therefore transferred each of the polar mutations into strain RP511, which carries the *rho-104* allele, and compared the chemotactic behavior of the resulting strains with that of the *rho*$^+$ parents (Fig. 2). All of the polar mutants regained chemotactic ability in the presence of *rho-104*, although some responded more dramatically than others. However, none of the mutant swarms exhibited the internal rings indicative of *tar* function. Since *rho* mutations alleviate polarity, but do not restore the function of the gene containing the polar mutation, these findings suggest that the six polar mutations lie within the *tar* gene.

Complementation analyses and fine structure mapping of these polar mutations were carried out to confirm that they were defective in *tar* function. To do these tests, each of the mutations was first transferred to RP4368, which carries the *tsr-1* mutation. The purpose of the *tsr* mutant background was to facilitate detection of complementation and recombination on swarm agar. Because loss of *tar* function alone does not preclude chemotaxis, it is often difficult to distinguish *tar* mutants from the wild type on swarm agar. As shown in Fig. 1, double mutants lacking both *tar* and *tsr* function are generally nonchemotactic. By analyzing *tar* mutations in a *tsr* background, the formation of *tar*$^+$ recombinants results in a change from a Che$^-$ to a Tsr$^-$ phenotype, which is readily detected on swarm agar. This mapping strategy should be applicable to any sort of *tar* mutation, including ones with polar properties.

The results of these genetic analyses are summarized in Table 2. All five polar mutants

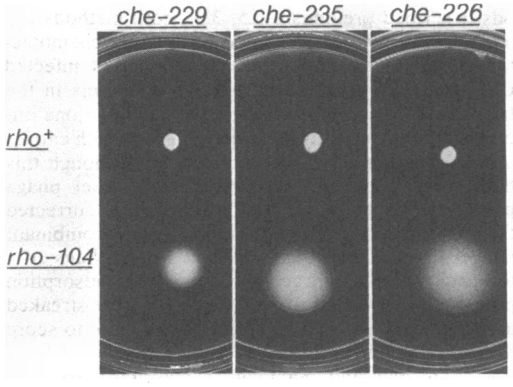

FIG. 2. Effect of Rho factor on the chemotactic behavior of polar *tar* mutants. Polar mutations were transferred into isogenic *rho*$^+$ and *rho-104* backgrounds, and individual colonies were incubated on tryptone swarm agar for 16 h at 35°C. Examples of three polar mutations, indicating the range of increased swarm sizes observed in the *rho*$^-$ background, are shown.

TABLE 2. Complementation analysis of polar *che* mutations

Recipient mutation[a]	Complementation[b] with transducing phages						
	None	52 (Tar^+R^+)	52Δ1 ($\Delta tarR^+$)	22 ($Tar^+R^+B^+Y^+Z^+$)	22Δ11 ($\Delta tarR^+B^+Y^+Z^+$)	52 (*che-235*)	52 (*che-252*)
che-226	0	R	0	+	0	R	R
che-229	0	R	0	+	0	R	R
che-235	0	R	0	+	0	0	R
che-252	0	R	0	+	0	R	0
che-256	0	R	0	+	0	R	R
Δtar-5201	0	+	0	+	0	0	0

[a] These mutations were transduced into RP4368 (*tsr-1*) to assess complementation for *tar* function, as discussed in the text.

[b] Symbols: (+) complementation, wild-type recombinants also formed; (R) no complementation, but wild type recombinants formed; 0, neither complementation nor recombination.

formed chemotactic (i.e., tar^+) recombinants with λfla52, but not with λfla52Δ1. Thus, the polar mutations must map within the segment missing in λfla52Δ1, which carries the *Δtar-5201* deletion. Even though λ*fla*52 carries a functional *tar* (and *cheR*) locus, it does not carry the *cheBYZ* genes and therefore was unable to complement the polar mutants because they also require *cheRBYZ* function for chemotaxis. Note that λche22 (tar^+ $cheRBYZ^+$) did complement these polar strains, whereas λche22Δ11 (tar^- $cheRBYZ^+$) did not. This result showed that in a *tsr* background restoration of *cheRBYZ* function in the polar mutants was not sufficient for chemotaxis, evidently because they still retained a defect in *tar* function due to the polar mutation.

Two of the polar mutations (*235* and *252*) were also transferred to λfla52 and then tested for ability to complement a *Δtar-5201 tsr-1* double mutant. Since the host strain in this test is able to express *cheRBYZ* function, it only requires *tar* function to regain chemotactic ability. Neither polar mutation could complement this tester strain (Table 2), again indicating a defect in *tar* function. The possibility that these mutations might be dominant when carried on λfla52 was ruled out by demonstrating that the mutant phage still complemented host mutants defective in other chemotaxis functions, for example, *cheA* and *cheW* (data not shown).

We also examined seven of the *tar* strains described by Reader et al. (26). These strains exhibited a variety of swarm sizes (Fig. 3); however, all of the swarms lacked the inner aspartate ring. We suspected that these differences in swarm size were due to differences in the genetic backgrounds of the strains, and therefore we transferred each *tar* mutation to strain RP437 by cotransduction with the *eda* locus. We found that all but one of the mutants exhibited a further decrease in swarm size when the mutation was transduced into RP437. This finding indicated that the original *tar* mutants probably harbored second-site mutations that influenced swarm size, but that much of the variability in swarm size was due to differences in the *tar* mutations themselves (or to mutations linked to the *tar* locus). When we lysogenized these RP437 *tar* derivatives with λche22Δ11, a transducing phage that carries and expresses the *cheRBYZ* functions, their swarm sizes increased substantially, but they still lacked the aspartate ring (Fig. 3). This result suggests that the small swarm size was due to reduced expression of the *cheRBYZ* genes, presumably as a consequence of polarity. Evidently, most of the original *tar* mutants contained polar mutations with second-site polarity suppressors.

Evidence for a "spacer region" between the *tar* and *cheR* loci. Parkinson and Houts (25) recently described the construction of λche22, a specialized transducing phage that carries the entire *tar* operon as well as an adjacent operon of chemo-

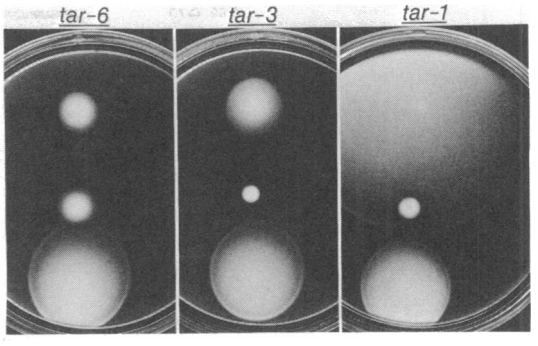

FIG. 3. Swarm phenotypes of *tar* alleles in various genetic backgrounds. Individual colonies of strains carrying the *tar* alleles described by Reader et al. (26) were inoculated on tryptone swarm plates and incubated at 35°C for 12 h. Examples of three *tar* alleles are shown. Top row, Mutations in their original genetic background; middle row, same mutations transduced into strain RP437; bottom row, RP437 *tar* derivatives made lysogenic for λche22Δ11, which supplies the *cheRBYZ* gene products at essentially wild-type levels.

taxis-related genes. In that study a large collection of λche22 deletion mutants was isolated and mapped against a series of host mutants, including the five polar *tar* strains described above. The results of that work are summarized in Fig. 4.

Many of the λche22 deletions shown in Fig. 4 appeared to be useful for further fine structure analysis of the *tar* region; 24 had an endpoint within the *tar* gene; 17 entered *tar* from the upstream side, but failed to recombine with the most promoter-distal *tar* allele, and yet retained *cheR* function; 7 others approached *tar* from the downstream side and removed all known *cheR* sites, yet complemented *tar* mutants. The high proportion of deletions with an endpoint at the *tar-cheR* border could be due to any one of several factors. First, there could be hot spots for deletion formation in this region. Second, there might be a nonrandom distribution of mutant alleles within the *tar* and *cheR* genes, producing a region devoid of mutational sites in which these deletion endpoints lie. Third, there could be a space between the *tar* and *cheR* coding regions. To test these various possibilities, we examined the physical sizes and positions of selected λche22 deletions by restriction site mapping.

The *E. coli* insert in λche22 is approximately 14 kilobase pairs in length; some of the restric-

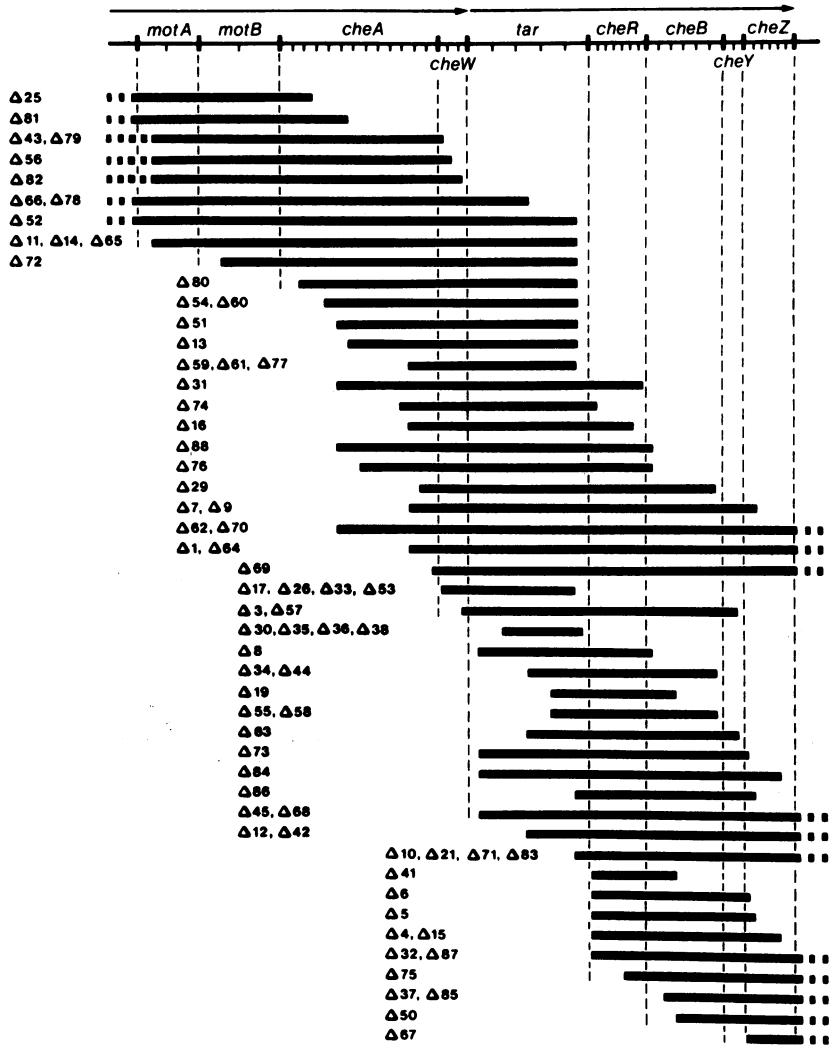

FIG. 4. Map of λche22 deletions. The positions of the deletion endpoints were determined by complementation and recombination tests against a series of host mutants (see reference 25). Deletion endpoints mapping within the *tar* gene or near the *tar* gene borders were used for further fine structure analysis of the *tar* region.

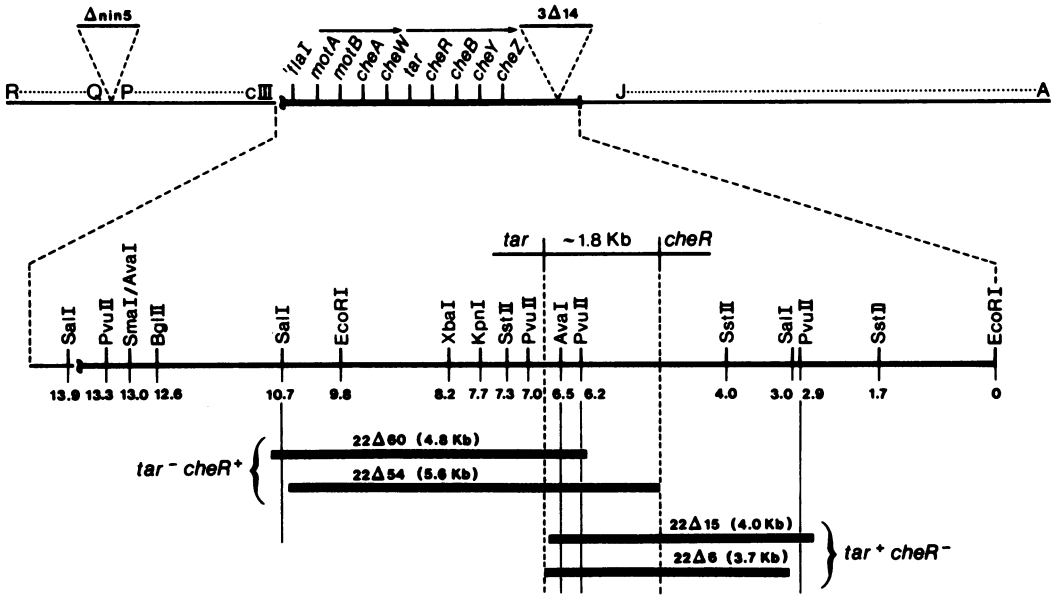

FIG. 5. Physical map of λche22. The positions of restriction endonuclease sites in the approximately 14-kb insert of λche22 were determined by digestion patterns of λ*che*22 and λche22 deletion phage. The physical location and size of four λche22 deletions that genetically mapped to the *tar-cheR* border are shown. The *cheR* gene lies to the right of the border defined by the right deletion endpoint of λche22Δ54 (*tar-cheR*$^+$). The *tar* gene lies to the left of the border defined by the left deletion endpoint of λche22Δ6 (*tar*$^+$ *cheR*$^-$). A region of approximately 1.8 kb lies between these borders.

tion endonuclease cleavage sites located within the insert are shown in Fig. 5. A number of λche22 deletion mutants with an endpoint at the *tar-cheR* border were examined for loss of restriction sites and changes in restriction fragment sizes. The most informative of those deletions are shown in Fig. 5. Mutants λche22Δ54 and λche22Δ60 were *tar*$^-$ *cheR*$^+$ in genetic tests; therefore the *cheR* gene must lie to the right of these deletions. Mutants λche22Δ6 and λche22Δ15 were *tar*$^+$ *cheR*$^-$, so the *tar* gene must lie to the left of these deletions. All four of these deletion mutants lacked two restriction sites in common, the *Pvu*II site at position 6.2 in the insert and the *Ava*I site at position 6.5 (Fig. 5). These results indicate that the deletions must overlap in a genetically silent region between the *tar* and *cheR* genes. We estimated from the relative physical positions of the deletion endpoints in λche22Δ6 and λche22Δ54 that this "silent region" was approximately 1.8 kilobases (kb) in extent. As we show below, most of the deletions that appeared to end at the *tar-cheR* border on the basis of genetic tests in fact have an endpoint within this 1.8-kb spacer region.

Identification of a new gene product encoded by the *tar* operon. The 1.8-kb spacer region between the *tar* and *cheR* genes represents 65 kilodaltons (kd) of protein coding capacity and could conceivably direct the synthesis of one or more gene products. To explore this possibility we examined protein synthesis in a series of λche22 deletion strains. Host cells lysogenic for a noninducible λ prophage were heavily irradiated with UV light and then infected with λche22 deletion strains to specifically label proteins synthesized from the *E. coli* inserts of the phages. Labeled proteins were then analyzed by sodium dodecyl sulfate-polyacrylamide gel electrophoresis and compared with the known chemotaxis gene products that had been identified in previous studies (Fig. 6) (32). The phage strains used in these experiments, their genetic content, and their protein products are summarized in Table 3.

The gel pattern of λche22 (Fig. 6) was consistent with previous work, although the *cheW* and *cheY* proteins were not seen under these gel conditions due to their small size. In addition, we noted that the *cheR* gene product (M_r, 28 kd) seemed to comigrate with another phage-directed protein that probably corresponds to the λ repressor (M_r, 27 kd). The complex series of bands of 60 to 65 kd was previously thought to represent only the *tar* gene product, which can exist in a variety of electrophoretic forms due to different methylation states as well as the presence or absence of a *cheB*-dependent post-translational modification (27, 29). However, the uppermost component of this band complex (Fig.

TABLE 3. Genetic content and protein products of λ transducing phages

Phage strain	Genes and gene products[a]									
	motA (31 kd)	*motB* (39 kd)	*cheA* (78 kd, 69 kd)	*cheW* (~15 kd)	*tar* (~60 kd)	*tap* (~65 kd)	*cheR* (24 kd)	*cheB* (38 kd)	*cheY* (~12 kd)	*cheZ* (24 kd)
λche22	+	+	+	+	+	+	+	+	+	+
Single deletions[b]										
Δ25, Δ43	−	−	−	−	+	+	+	+	+	+
Δ11	F	−	−	−	F	+	+	+	+	+
Δ5	+	+	+	+	+	F	−	−	−	F
Δ37	+	+	+	+	+	+	+	−	−	−
Double deletions[c]										
Δ25–Δ5	−	−	−	−	+	F	−	−	−	F
Δ43–Δ37	−	−	−	−	+	+	+	−	−	−
Δ11–Δ37	F	−	−	−	F	+	+	−	−	−

[a] Genetic content was defined by complementation tests, except in the case of *tap*, whose presence can only be inferred from deletion mapping. Gene products were detected by UV programming, as explained in the text. Symbols: (+) both complementation activity and the associated gene product were observed; (−) neither gene function nor a gene product was observed (in some cases, e.g., λche22Δ25, genes are present, but inactive due to absence of an active promoter [25]); (F) genes containing deletion endpoints that resulted in the production of a fusion protein.

[b] These strains are derivatives of λche22 [25].

[c] These strains were constructed by crossing two λche22 deletion strains as described in the text.

6) behaved independently of the lower bands in the complex and did not appear to be correlated with the presence of *tar* activity, but rather with the spacer region between the *tar* and *cheR* genes.

The spacer region band was present in λche22Δ11 (Fig. 6), whereas the lower bands of the complex were not. This phage carries a deletion between the *motA* and *tar* genes and does not express *tar* function in complementation tests. This phage did produce a novel product (M_r, 45 kd) that probably represents a *motA-tar* fusion protein. The spacer region band was not made by λche22Δ5 (Fig. 6), which is deleted between the spacer region and *cheZ*. This phage did, however, synthesize the lower bands associated with *tar* function as well as an apparent spacer region-*cheZ* fusion protein that comigrated with the small *cheA* product (M_r, 69 kd).

The assignment of the 65-kd protein to the spacer region was confirmed with the aid of several recombinant λche22 strains in which most of the extraneous chemotaxis functions were deleted. For example, λche22Δ25-Δ5 expresses only *tar* activity and synthesizes the 60 to 63-kd *tar* bands and the spacer-*cheZ* fusion protein (Fig. 6). λche22Δ43-Δ34 makes only the *tar* and *cheR* product in addition to the spacer region band, and λche22Δ11-Δ37 makes only the spacer region band and the *cheR* product in addition to the *motA-tar* fusion protein (Fig. 6).

Our UV programming experiments thus demonstrated that the *tar-cheR* spacer region made a protein product of approximately 65 kd. This product size would require a coding region of about 1.8 kb, which corresponds closely to the estimated length of the spacer region. It seems unlikely, therefore, that any additional gene products are made from this region. Recently, two other groups independently reported the discovery of a 65-kd protein encoded by the *tar-cheR* region (3, 42). Boyd et al. (4) designated this region as the *tap* locus and its product as a "taxis-associated protein." We assume that the protein we observed is the *tap* product, and we will adopt this terminology for the remainder of our article.

Isolation and mapping of insertion mutations in *tar* and *tap*. None of the point mutations in our mutant collection has been mapped to the *tap* gene, suggesting that *tap* defects may have little or no effect on chemotactic ability, at least as it is measured in tryptone swarm plates. Since the *tap* locus is part of the *tar* operon and lies upstream from the *cheRBYZ* genes, it should be possible to identify polar mutations in the *tap* gene by virtue of their expected Che^- phenotype. We therefore isolated and characterized a large number of nonchemotactic mutants generated by Mu *d*1 mutagenesis. This phage inserts essentially at random into the *E. coli* chromosome and causes a virtually complete polar block on expression of promoter-distal functions (5).

Approximately 150 nonchemotactic Mu *d*1-induced mutants were isolated and characterized with a set of λ transducing phages. Mutants that were complemented by λche22Δ82 (Δ*motA-cheW*; Fig. 4), and that gave chemotactic recombinants with λche22Δ75 (Δ*cheR-cheZ*; Fig. 4), were assumed to have insertions in the *tar-tap* region. A total of 31 mutants with *tar-tap* inser-

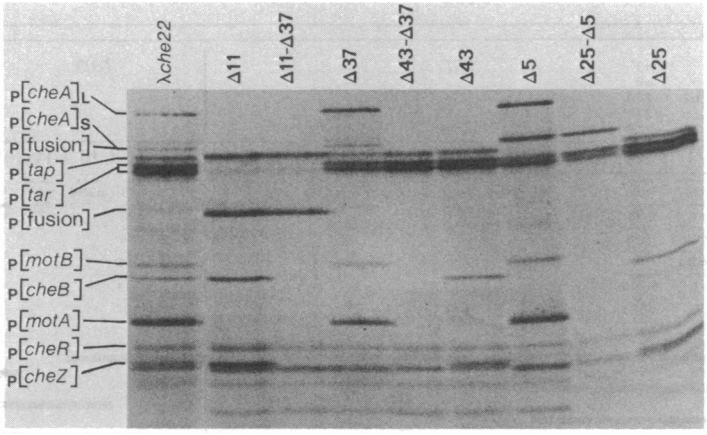

FIG. 6. Polypeptide products of the *tar* operon. λche22 strains (Table 3) were used to radiolabel chemotaxis gene products by UV programming (33). Shown is an autoradiogram of an 11% polyacrylamide gel containing 0.8% sodium dodecyl sulfate. Gene product identifications are based on the genetic content of the various phage strains (Table 3) and the assignments given in references 32 and 33. Fusion proteins produced by the Δ11 and Δ5 deletions are designated p[fusion]. p[tap] indicates a 65-kd polypeptide correlated with the region located between the *tar* and *cheR* genes (see the text).

tions were obtained; 19 of them had a Lac^+ phenotype, indicating that the *lac* genes of the prophage were inserted in the correct orientation for transcription by the *tar* promoter.

Each of these Mu *d*1 insertions was mapped against a series of deleted λ transducing phages (Fig. 7). Deletions that failed to express *cheRBYZ* function, i.e., those entering the *tar-tap* region from the downstream (*cheR*) side, as well as polar deletions entering from the upstream side, were unable to complement the chemotaxis defects of the Mu *d*1 insertion mutants. Such deletions gave chemotactic recombinants only if they did not overlap the insertion site. Nonpolar deletions entering the *tar-tap* region from the upstream side could not be used for mapping, because, by supplying *cheRBYZ* function, they were able to complement polar mutants for chemotaxis even in cases where the deletion clearly overlapped the insertion site. Deletions of this sort could be used, however, to establish the position of the *tar-tap* border relative to the Mu *d*1 insertion sites. For example, λche22Δ11 is functionally tar^- tap^+, as shown by the UV programming experiments discussed above. Polar insertions in *tar*, when complemented by λche22Δ11, should therefore have a Tar^- phenotype, whereas *tap* insertions should be fully complemented to the wild type. In fact, the Mu *d*1 insertion strains fell into these two expected groups in the complementation tests, thus defining the *tar-tap* gene border (Fig. 7). When similar tests were performed with phage deletions that removed both *tar* and *tap* function (e.g., λche22Δ13; Fig. 7), the results were identical to those with λche22Δ11; *tar* insertions had a Tar^- phenotype, and *tap* insertions had a wild-type phenotype. This observation demonstrated that absence of *tap* function did not cause a detectable change in swarm morphology on semisolid tryptone agar.

Since *tap* defects produced no discernible phenotype, the relative endpoints of deletions entering *tap* from the upstream side (e.g., λche22Δ13; Fig. 7) could not be established by genetic mapping. We were able, however, to map two nonpolar upstream deletions ending in *tar* (λche22Δ11, λche22Δ80) by phage-phage crosses in RP3808. This host carries a *tsr* mutation and an extensive deletion that removes all of the *tar* locus. Phage deletions that enter *tar* from opposite sides and do not overlap should be able to form Che^+ (i.e., Tar^+) recombinants in this host by first recombining with each other to generate a tar^+ phage. In this manner we established that λche22Δ11 overlapped λche22Δ55 and λche22Δ71, but not λche22Δ21, λche22Δ86, or any shorter deletions entering *tar* from the downstream side. Similarly, λche22Δ80 failed to recombine with λche22Δ19, but did recombine with λche22Δ58, λche22Δ83, and shorter deletions (Fig. 4). All phage-phage combinations of this sort involving deletions ending in *tap* produced Che^+ recombinants, presumably because one of the two deletions was necessarily tar^+ in such crosses. This result indicates that *tsr tap* mutants, unlike *tsr tar* mutants, do not have a generally nonchemotactic phenotype.

Physical map of the *tar* region. A number of the phage deletions that had been shown by genetic mapping to end in the *tar-tap* region (Fig. 7) were also positioned physically by restriction endonuclease analysis. The resultant physical

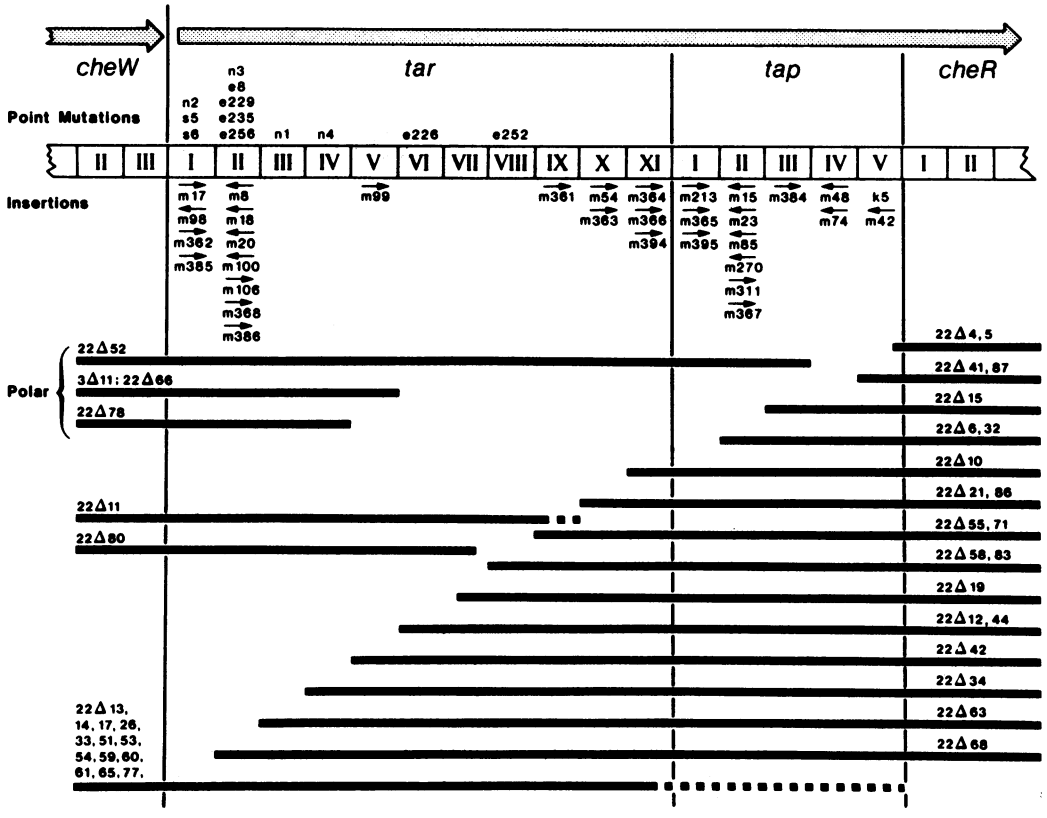

FIG. 7. Genetic map of the *tar* region. The relative positions of mutations and deletion endpoints were determined by recombination tests between mutant host strains and λche22 deletion derivatives. The positions of several deletion endpoints relative to one another were also established by phage-phage crosses as described in the text. The origin of the mutant alleles is indicated by the letter prefix as follows: n, *N*-methyl-*N*-nitrosoguanidine-induced mutants; e, ethyl methane sulfonate-induced mutations; s, spontaneous mutations; m, Mu *d*1 insertions; k, Tn*5* insertion. The arrows above the Mu *d*1 insertions indicate the orientation of the insertion based on Lac^+ (→) or Lac^- (←) phenotype.

map is presented in Fig. 8. In constructing this map, we also utilized recombinant plasmids containing restriction fragments derived from the bacterial insert of λche22. The genetic content of these plasmid clones was determined by transformation of a series of host tester mutants and enabled us to localize various restriction sites to particular chemotaxis genes. The endpoints of the λche22 deletions could then be positioned with a fair degree of accuracy by considering their physical extent (as measured by changes in restriction fragment lengths), the restriction sites they removed, and their relative genetic endpoints. Finally, we positioned the chemotaxis genes on our physical map by using the known sizes of their protein products to estimate their lengths in kilobase pairs. There appears to be little unused coding capacity throughout the *motA-cheZ* interval (Fig. 8), and it seems unlikely that there could be any other genes in this region.

DISCUSSION

The *tar* gene (MCPII) appears to play several roles in *E. coli* chemotaxis: it serves as the chemoreceptor for aspartate stimuli (41), it handles maltose stimuli by interacting with occupied maltose binding protein (14), it controls flagellar rotation in response to both aspartate and maltose stimuli (18); and it undergoes methylation-demethylation to bring about sensory adaptation (31, 34). To understand these various functions and their underlying molecular basis, we have initiated a detailed genetic analysis of the *tar* locus to explore structure-function relationships within the *tar* gene product.

In this article, we investigated the genetic properties of the few known *tar* mutants and isolated a number of additional *tar* mutants by insertion mutagenesis with the Mu *d*1 element. We also characterized the transcriptional and physical organization of the *tar* region by com-

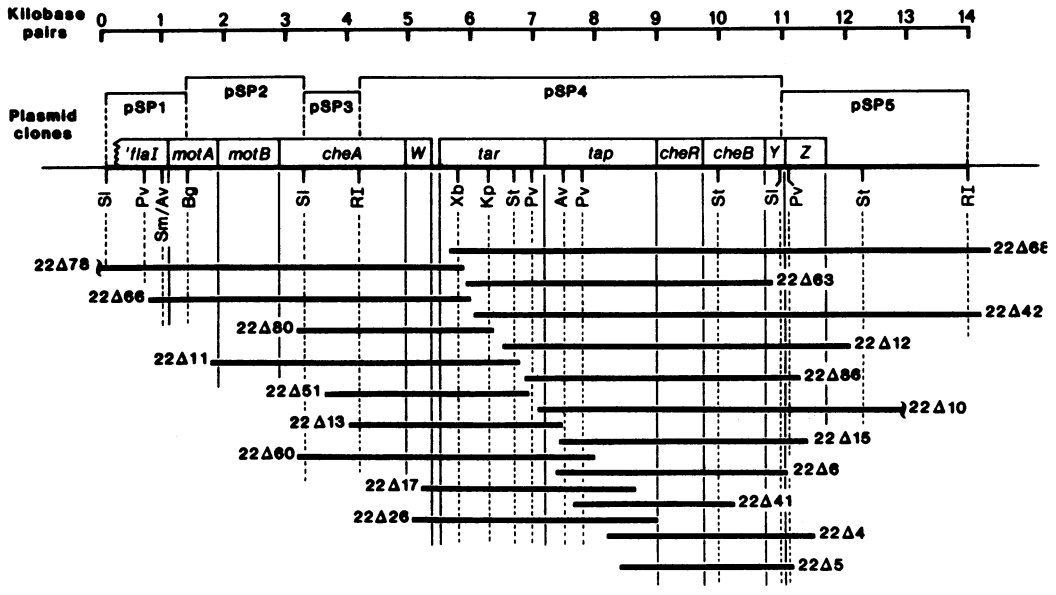

FIG. 8. Physical map of λche22. The location and size of phage deletions with endpoints in the *tar-tap* region are based on restriction endonuclease analysis. The physical sizes of the chemotaxis genes are based on the sizes of their protein products; their positions are based on the genetic content of deletion phage and plasmid clones. Abbreviations used for restriction endonuclease cleavage sites: Av, *Ava*I; Bg, *Bgl*II; Kp, *Kpn*I; Pv, *Pvu*II; RI, *Eco*RI; Sl, *Sal*I; Sm, *Sma*I; St, *Sst*II; Xb, *Xba*I.

plementation analysis, fine structure mapping, and DNA restriction fragment mapping. In addition to laying the necessary groundwork for subsequent genetic work, these studies revealed several new features of the *tar* region.

Transcriptional organization. All Mu *d*1 insertions, as well as some point mutations in the *tar* gene, exhibited a generally nonchemotactic phenotype. Complementation tests indicated that this was due to polar effects on transcription of the adjacent *cheRBYZ* genes. Similar polarity effects were seen in deletions lacking the amino-terminal coding region of *tar*, suppporting the notion that the *tar* and *cheRBYZ* genes form a transcriptional unit whose promoter lies at the upstream end of the *tar* locus. These findings are consistent with the properties of Tn*5* insertions in *tar* reported by Boyd et al. (3), but, in addition, rule out the possibility that the *tar* function itself is somehow required for the expression of other chemotaxis genes.

Most of the *tar* mutations described by Reader et al. (26) proved to have at least partial polar effects on downstream *che* gene expression and are therefore not suitable for structure-function analyses, because they probably make a grossly altered product. The original strains in which these mutations were isolated appear to have acquired secondary mutations that in most instances have suppressed the polarity effects of the *tar* lesions. It seems likely that these mutants were somehow favored by the selection method used to isolate them. For example, some of the strains were obtained by repeatedly cycling the bacteria left at the origin on swarm plates, which would enrich for generally nonchemotactic mutants. Subsequent selection for "good motility" could have given rise to the polarity suppressors.

***Tap* locus.** We obtained several lines of evidence for the existence of a new chemotaxis-related gene located between the *tar* and *cheR* loci. Physical maps of this region revealed approximately 1.8 kb of potential coding capacity between the downstream *tar* border and the upstream *cheR* border, sufficient to encode a protein of 65 kd. A product of this size was observed in UV programming experiments with specialized transducing phages and was correlated with the presence of the 1.8-kb region. Both Boyd et al. (3) and Wang et al. (42) have independently discovered the same gene. We used the name *tap* (taxis-associated protein) for this new locus (3).

Physical measurements of plasmids covering the *tar* region had previously indicated that essentially all of the coding capacity could be accounted for by known genes and gene products (21). The *tap* locus may have been overlooked in those studies due to relatively small errors in plasmid length measurements coupled with the fact that the *tar* and *tap* products are

similar in both size and banding pattern on sodium dodecyl sulfate-polyacrylamide gel electrophoresis and would have been difficult to distinguish without the aid of appropriate deletion or insertion mutants. Our physical measurements, based on restriction mapping, indicate that the *tar* region should now be saturated, and it is unlikely that there are any undiscovered genes between the *tar* and *cheZ* loci. It is still possible that other chemotaxis-related genes are located downstream of *cheZ*, but none has yet been detected, in spite of extensive mutant hunts.

The main reason why *tap* remained undiscovered until recently is that mutants lacking the *tap* function are not demonstrably defective in chemotaxis. It has been suggested that the *tap* and *tar* loci have homologous functions (42), but we have not been able to support this idea. For example, deletion mutants lacking the *tar* function have a characteristic Tar^- phenotype, whereas those lacking the *tap* function have a wild-type phenotype. It is possible that *tap* has some subtle role in chemotaxis or is needed for responses to chemical stimuli that have not yet been tested. These questions will be dealt with in more detail in a subsequent publication.

ACKNOWLEDGMENTS

This work was supported by Public Health Service grant GM-19559 from the National Institute of General Medical Sciences. M.K.S. was supported by a Public Health Service predoctoral traineeship GM-07464 from the National Institute of General Medical Sciences.

Some of the Mu *d*1 insertion mutants used in this study were isolated by Paul Talbert. Parts of this work were carried out by J.S.P. while on sabbatical leave at the European Molecular Biology Laboratory, Heidelberg, West Germany, and he thanks Noreen Murray for her kind hospitality and patient encouragement.

LITERATURE CITED

1. **Berg, H. C., and D. A. Brown.** 1972. Chemotaxis in *Escherichia coli* analyzed by three-dimensional tracking. Nature (London) **239**:500–504.
2. **Berg, H. C., and P. M. Tedesco.** 1975. Transient response to chemotactic stimuli in *Escherichia coli*. Proc. Natl. Acad. Sci. U.S.A. **72**:3235–3239.
3. **Boyd, A., A. Krikos, and M. Simon.** 1981. Sensory transducers of *E. coli* are encoded by homologous genes. Cell **26**:333–343.
4. **Boyd, A., and M. I. Simon.** 1980. Stimulus-elicited methylation generates multiple electrophoretic forms of methyl-accepting chemotaxis proteins in *Escherichia coli*. J. Bacteriol. **143**:809–815.
5. **Casadaban, M. J., and S. N. Cohen.** 1979. Lactose genes fused to exogenous promoters in one step using a Mu-*lac* bacteriophage: in vivo probe for transcriptional control sequences. Proc. Natl. Acad. Sci. U.S.A. **76**:4530–4533.
6. **Chelsky, D., and F. W. Dahlquist.** 1980. Structural studies of methyl-accepting chemotaxis proteins of *Escherichia coli*: evidence for multiple methylation sites. Proc. Natl. Acad. Sci. U.S.A. **77**:2434–2438.
7. **Davis, R. W., D. Botstein, and J. R. Roth.** 1980. A manual for genetic engineering, advanced bacterial genetics. Cold Spring Harbor Laboratory, Cold Spring Harbor, N.Y.
8. **DeFranco, A. L., and D. E. Koshland, Jr.** 1980. Multiple methylation in the processing of sensory signals during bacterial chemotaxis. Proc. Natl. Acad. Sci. U.S.A. **77**:2429–2433.
9. **Engstrom, P., and G. L. Hazelbauer.** 1980. Multiple methylation of methyl-accepting chemotaxis proteins during adaptation of *E. coli* to chemical stimuli. Cell **20**:165–171.
10. **Hedblom, M. L., and J. Adler.** 1980. Genetic and biochemical properties of *Escherichia coli* mutants with defects in serine chemotaxis. J. Bacteriol. **144**:1048–1060.
11. **Ish-Horowicz, D., and J. F. Burke.** 1981. Rapid and efficient cosmid cloning. Nucleic Acids Res. **9**:2989–2998.
12. **Kihara, M., and R. M. Macnab.** 1981. Cytoplasmic pH mediates pH taxis and weak-acid repellent taxis of bacteria. J. Bacteriol. **145**:1209–1221.
13. **Kleene, S. J., M. L. Toews, and J. Adler.** 1977. Isolation of glutamic acid methyl ester from an *Escherichia coli* membrane protein involved in chemotaxis. J. Biol. Chem. **252**:3214–3218.
14. **Koiwai, O., and H. Hayashi.** 1979. Studies on bacterial chemotaxis. IV. Interaction of maltose receptor with a membrane-bound chemosensing component. J. Biochem. (Tokyo) **86**:27–34.
15. **Komeda, Y., and T. Iino.** 1979. Regulation of the expression of the flagellin gene (*hag*) in *Escherichia coli* K-12: analysis of *hag-lac* gene fusions. J. Bacteriol. **139**:721–729.
16. **Kondoh, H., C. B. Ball, and J. Adler.** 1979. Identification of a methyl-accepting chemotaxis protein for the ribose and galactose chemoreceptors of *Escherichia coli*. Proc. Natl Acad. Sci. U.S.A. **76**:260–264.
17. **Laemmli, U. K.** 1970. Cleavage of structural proteins during assembly of the head of bacteriophage T4. Nature (London) **227**:680–685.
18. **Larsen, S. H., R. W. Reader, E. N. Kort, W.-W. Tso, and J. Adler.** 1974. Change in direction of flagellar rotation is the basis of the chemotactic response in *Escherichia coli*. Nature (London) **249**:74–77.
19. **Macnab, R. W., and D. E. Koshland, Jr.** 1972. The gradient-sensing mechanism in bacterial chemotaxis. Proc. Natl. Acad. Sci. U.S.A. **69**:2509–2512.
20. **Maeda, K., and Y. Imae.** 1979. Thermosensory transduction in *Escherichia coli*: inhibition of the thermoresponse by L-serine. Proc. Natl. Acad. Sci. U.S.A. **76**:91–95.
21. **Matsumura, P., M. Silverman, and M. Simon.** 1977. Synthesis of *mot* and *che* gene products of *Escherichia coli* programmed by hybrid ColE1 plasmids in minicells. J. Bacteriol. **132**:996–1002.
22. **Parkinson, J. S.** 1976. *cheA*, *cheB*, and *cheC* genes of *Escherichia coli* and their role in chemotaxis. J. Bacteriol. **126**:758–770.
23. **Parkinson, J. S.** 1978. Complementation analysis and deletion mapping of *Escherichia coli* mutants defective in chemotaxis. J. Bacteriol. **135**:45–53.
24. **Parkinson, J. S.** 1980. Novel mutations affecting a signaling component for chemotaxis of *Escherichia coli*. J. Bacteriol. **142**:953–961.
25. **Parkinson, J. S., and S. E. Houts.** 1982. Isolation and behavior of *Escherichia coli* deletion mutants lacking chemotaxis functions. J. Bacteriol. **151**:106–113.
26. **Reader, R. W., W.-W. Tso, M. S. Springer, M. F. Goy, and J. Adler.** 1979. Pleiotropic aspartate taxis and serine taxis mutants of *Escherichia coli*. J. Gen. Microbiol. **111**:363–374.
27. **Rollins, C. and F. W. Dahlquist.** 1981. The methyl-accepting chemotaxis proteins of *E. coli*: a repellent-stimulated, covalent modification, distinct from methylation. Cell **25**:333–340.
28. **Segall, J. E., M. D. Manson, and H. C. Berg.** 1982. Signal processing times in bacterial chemotaxis. Nature (London) **296**:855–857.
29. **Sherris, D., and J. S. Parkinson.** 1981. Post-translational processing of methyl-accepting chemotaxis proteins in *Escherichia coli*. Proc. Natl. Acad. Sci. U.S.A. **78**:6051–6055.

30. **Silverman, M., and M. Simon.** 1974. Flagellar rotation and the mechanism of bacterial motility. Nature (London) **249**:73–74.
31. **Silverman, M., and M. Simon.** 1977. Chemotaxis in *Escherichia coli*: methylation of *che* gene products. Proc. Natl. Acad. Sci. U.S.A. **74**:3317–3321.
32. **Silverman, M., and M. Simon.** 1977. Identification of polypeptides necessary for chemotaxis in *Escherichia coli*. J. Bacteriol. **130**:1317–1325.
33. **Smith, R. A., and J. S. Parkinson.** 1980. Overlapping genes at the *cheA* locus of *Escherichia coli*. Proc. Natl. Acad. Sci. U.S.A. **77**:5370–5374.
34. **Springer, M. S., M. F. Goy, and J. Adler.** 1977. Sensory transduction in *Escherichia coli*: two complementary pathways of information processing that involve methylated proteins. Proc. Natl. Acad. Sci. U.S.A. **74**:3312–3316.
35. **Springer, M. S., E. N. Kort, S. H. Larsen, G. O. Ordal, R. W. Reader, and J. Adler.** 1977. Role of methionine in bacterial chemotaxis: requirement for tumbling and involvement in information processing. Proc. Natl. Acad. Sci. U.S.A. **72**:4640–4644.
36. **Springer, W. R., and D. E. Koshland, Jr.** 1977. Identification of a protein methyltransferase as the *cheR* gene product in the bacterial sensing system. Proc. Natl. Acad. Sci. U.S.A. **74**:533–537.
37. **Spudich, J. L., and D. E. Koshland, Jr.** 1975. Quantitation of the sensory response in bacterial chemotaxis. Proc. Natl. Acad. Sci. U.S.A. **72**:710–713.
38. **Stock, J. B., and D. E. Koshland, Jr.** 1978. A protein methylesterase involved in bacterial sensing. Proc. Natl. Acad. Sci. U.S.A. **75**:3659–3663.
39. **Tso, W.-W., and J. Adler.** 1974. Negative chemotaxis in *Escherichia coli*. J. Bacteriol. **118**:560–576.
40. **VanDerWerf, P., and D. E. Koshland, Jr.** 1977. Identification of a γ-glutamylmethyl ester in a bacterial membrane protein involved in chemotaxis. J. Biol. Chem. **252**:2793–2795.
41. **Wang, E. A., and D. E. Koshland, Jr.** 1980. Receptor structure in the bacterial sensing system. Proc. Natl. Acad. Sci. U.S.A. **77**:7157–7161.
42. **Wang, E. A., K. L. Mowry, D. O. Clegg, and D. E. Koshland, Jr.** 1982. Tandem duplication and multiple functions of a receptor gene in bacterial chemotaxis. J. Biol. Chem. **257**:4673–4676.